

Electronic Supplementary Information (ESI)

Bio-inspired Nickel-Iron based organogel: An efficient and stable bifunctional electrocatalyst for overall water splitting in high current density

Debasish Ghosh,^a Subhransu Maharana,^a AsitBaran Panda ^{ab}*

^a Functional Materials Group, Advanced Materials and Corrosion Division, National Metallurgical Laboratory (CSIR-NML), Jamshedpur, Jharkhand, India, 831007.

^bAcademy of Scientific & Innovative Research (AcSIR), Ghaziabad, Uttar Pradesh- 201002.

Supporting Experimental details.

Solvent optimization test for all the synthesized NiFe-gel.

Various solvents, ranging from polar to non-polar, were tested for their ability to form gels with the chemical components of the synthesized NiFe-gels. Solvents such as water, methanol, ethanol, ethyl acetate, DMSO, DMF, THF, acetone, toluene, and benzene were used to evaluate their gelation capabilities. The stoichiometric amounts of gel-constituting agents, including metal salts and the gelator, were maintained according to the minimum critical gelation concentrations for each solvent, as required for the metallogelation studies. The gelation process, outlined in the experimental section, was followed for each solvent-directed attempt. The 'inversion-vial' test was performed for each case, and the results of the individual solvent-based experiments are presented in Table S1. The experimental results clearly indicate that a DMF:Water (1:1) mixture is the optimal solvent combination needed to achieve stable metallogels under the given experimental conditions.

Table S1. Gelation process of NiFe(1:1)-Gel in various solvents.

Entry	Solvent	Phase	Picture
1.	H ₂ O	No-Gel	
2.	MeOH	No-Gel	
3.	EtOH	No-Gel	
4.	EtOAc	No-Gel	
5.	DMSO	No-Gel	
6.	DMF	No-Gel	
7.	THF	No-Gel	
8.	Acetone	No-Gel	
9.	Toluene	No-Gel	

10.	Benzene	No-Gel	
11.	DMF:H ₂ O (1:1)	Gel	

Gelation tests were performed following the synthetic method discussed in the Experimental Section. Solvent abbreviations: H₂O = Water, MeOH = Methanol, EtOH = Ethanol, EtOAc = Ethyl Acetate, DMSO = Dimethyl sulfoxide, THF = Tetrahydrofuran and DMF = Dimethyl formamide.

Table S2. Gelation process of NiFe(1:1)-Gel in various counter ions.

Entry	Metal Salts	Solvent	Phase
1	NiCl ₂ and Fe(NO ₃) ₃	DMF:H ₂ O	No-Gel
2	NiSO ₄ and Fe(NO ₃) ₃	DMF:H ₂ O	No-Gel
3	NiCO ₃ and Fe(NO ₃) ₃	DMF:H ₂ O	No-Gel
4	Ni ₃ (PO ₄) ₂ and Fe(NO ₃) ₃	DMF:H ₂ O	No-Gel

Turnover Frequency (TOF) from OER Current Density

The turnover frequencies (TOF) for various catalyst variants, including Ni-Gel, Fe-Gel, NiFe(0.5:1)-Gel, NiFe(1.5:1)-Gel, and NiFe(1:1)-Gel, were calculated from the re-dox area of cyclic voltammograms (CV), which provides information on the electrochemically active atoms present in the catalyst. As shown in Fig. S7, the reduction area corresponds to the electrochemical activity. The TOF value for NiFe(1:1)-Gel (4.50 S^{-1}) is significantly higher than those of the other catalysts: Ni-Gel (0.06 S^{-1}), Fe-Gel (0.03 S^{-1}), NiFe(0.5:1)-Gel (0.43 S^{-1}), and NiFe(1.5:1)-Gel (0.50 S^{-1}). Therefore, NiFe(1:1)-Gel demonstrates superior catalytic activity, producing a higher number of oxygen molecules per unit time compared to the other catalysts.

TOF in our study was calculated assuming that the surface-active Metal ions that had undergone the redox reaction just before onset of OER only participated in OER electrocatalysis. The corresponding expression is

$$\text{TOF} = (j \times N_A) / (F \times n \times \Gamma) \quad (1)$$

Where, j = current density, N_A = Avogadro number, F = Faraday constant, n = Number of electrons transferred during the reaction, Γ = Surface concentration of the catalyst.

Calculated area associated with the reduction of M^{3+} to M^{2+} of **NiFe (1:1)-gel** = 0.000083751 VA .

$$\begin{aligned} \text{Hence, the associated charge is} &= 0.000083751 \text{ VA} / 0.005 \text{ Vs}^{-1} \\ &= 0.0167502 \text{ As} \\ &= 0.0167502 \text{ C} \end{aligned}$$

$$\begin{aligned} \text{Now, the number of electron transferred is} &= 0.0167502 \text{ C} / (1.602 \times 10^{-19} \text{ C}) \\ &= 1.04 \times 10^{17} \end{aligned}$$

Since, the reduction of M^{3+} to M^{2+} is a single electron transfer process, hence, the number of electrons calculated above is exactly same with the number of surface-active sites.

Hence, the number of M active sites participating in OER is $= 1.04 \times 10^{17}$

Therefore, surface concentration of the **NiFe (1:1)-gel** is $= 1.04 \times 10^{17}$

The current density at 1.42V potential was evaluated from the backward LSV curve of **NiFe (1:1)-gel.**

Hence, from equation (1)

$$\begin{aligned}\text{TOF}_{1.42\text{ V}} &= (300 \times 10^{-3}) \times (6.022 \times 10^{23}) / (96485 \times 4 \times 1.04 \times 10^{17}) \\ &= 4.50\text{ s}^{-1}\end{aligned}$$

Table S3. The summarized calculated TOF of the synthesized samples.

Catalysts	TOF _{1.42 V}
NiFe(1:1)-Gel	4.50 s⁻¹
NiFe(1.5:1)-Gel	0.43 s⁻¹
NiFe(0.5:1)-Gel	0.15 s⁻¹
Ni-Gel	0.06 s⁻¹
Fe-Gel	0.03 s⁻¹

Faradic efficiency

Faradic efficiency: Faradic efficiency was calculated using the Eq. (1)

$$\text{Faradic efficiency} = \frac{\text{experimental }\mu\text{mol of } O_2 \text{ gas}}{\text{theoretical }\mu\text{mol of } O_2 \text{ gas}} \times 100 \quad (1)$$

The theoretical amount of O₂ gas was calculated from Faraday's law

$$n = \frac{I \times t}{z \times F} \quad (2)$$

$$= \frac{0.5 \times 3600}{4 \times 96484}$$

$$= 4663 \mu\text{mol}$$

Where n is the number of mol, I is the current in ampere, t is the time in second, z is the transfer of electrons (for $\text{O}_2 = 4$), and F is the faraday constant (96485 C mol^{-1}).

The theoretical amount of O_2 gas after 1hour stability= $4663 \mu\text{mol}$

The experimental amount of gas ($\text{H}_2 + \text{O}_2$) was evaluated from the water displacement method.

Finally, the mole of gas ($\text{H}_2 + \text{O}_2$) produced in water displacement is calculation by the Eq.(3)

$$PV = nRT \quad (3)$$

V is the volume of produced gas in liters, T is the temperature in Kelvin, and R is the ideal gas constant ($0.0821 \text{ L atm/mol K}$)

The number of mol gas ($\text{H}_2 + \text{O}_2$) produced in water displacement after 1hour stability:

$$(1\text{atm})(0.3505\text{L}) = n (0.0821 \text{ L atm/ mol K}) (298\text{K})$$

$$n = \frac{(1 \text{ atm}) \times (0.3505\text{L})}{(0.082 \text{ Latm/ molK}) \times (308 \text{ K})}$$

$$n = 13877 \mu\text{mol}$$

Ratio of H_2 : $\text{O}_2 = 2:1$

$$\text{O}_2 = 13877 \times \frac{1}{3}$$

$$= 4625 \mu\text{mol}$$

Faradic efficiency after 1 hour stability:

$$\begin{aligned} \text{Faradicefficiency} &= \frac{4625 \mu\text{mol}}{4663 \mu\text{mol}} \times 100 \\ &= 99.1 \% \end{aligned}$$

The number of mole gas ($\text{H}_2 + \text{O}_2$) produced in water displacement after 100 hours stability:

$$(1\text{atm})(0.3505\text{L}) = n (0.0821 \text{ L atm/mol K}) (298\text{K})$$

$$n = \frac{(1 \text{ atm}) \times (0.3497\text{L})}{(0.082 \text{ Latm/molK}) \times (308 \text{ K})}$$

$$n = 13846 \mu\text{mol}$$

Ratio of H_2 : $\text{O}_2 = 2:1$

$$\text{O}_2 = 13846 \times \frac{1}{3}$$

$$= 4615 \mu\text{mol}$$

Faradic efficiency after 100 hours stability:

$$\begin{aligned} \text{Faradicefficiency} &= \frac{4615 \mu\text{mol}}{4663 \mu\text{mol}} \times 100 \\ &= 98.5 \% \end{aligned}$$

Supporting Figures

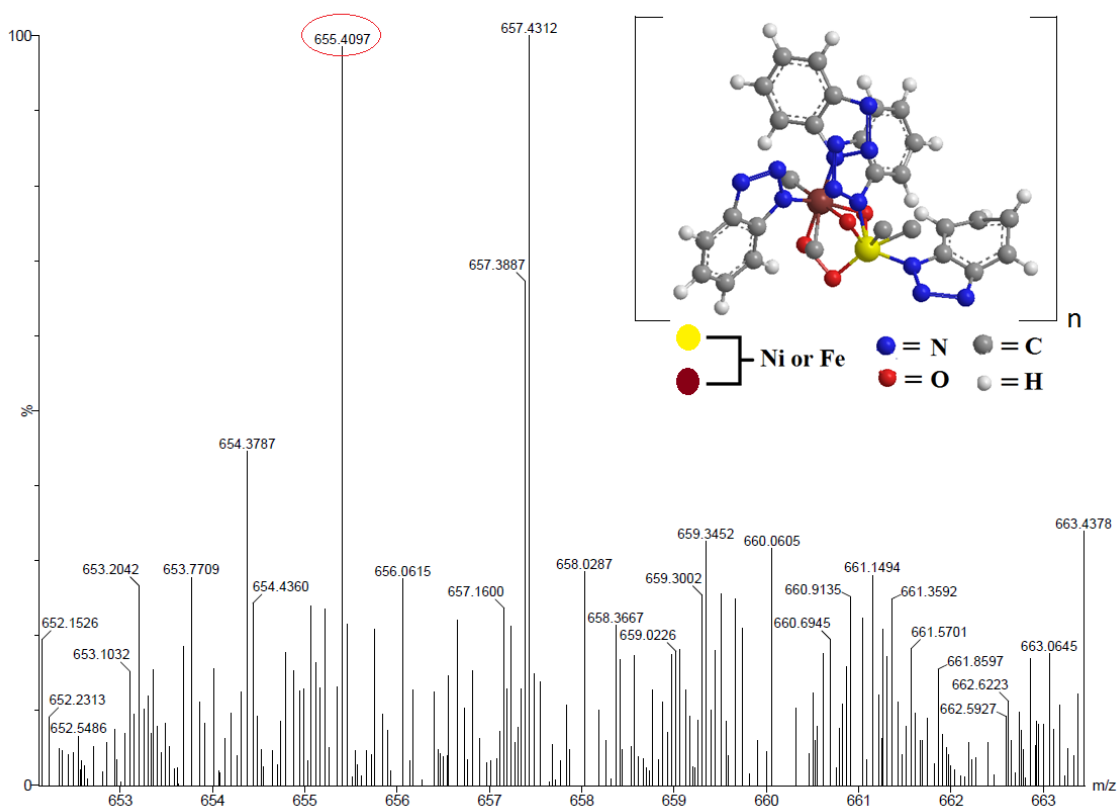


Fig. S1 HRMS spectrum of NiFe(1:1)-Gel having $[M + H]^+$ peak at m/z 655.

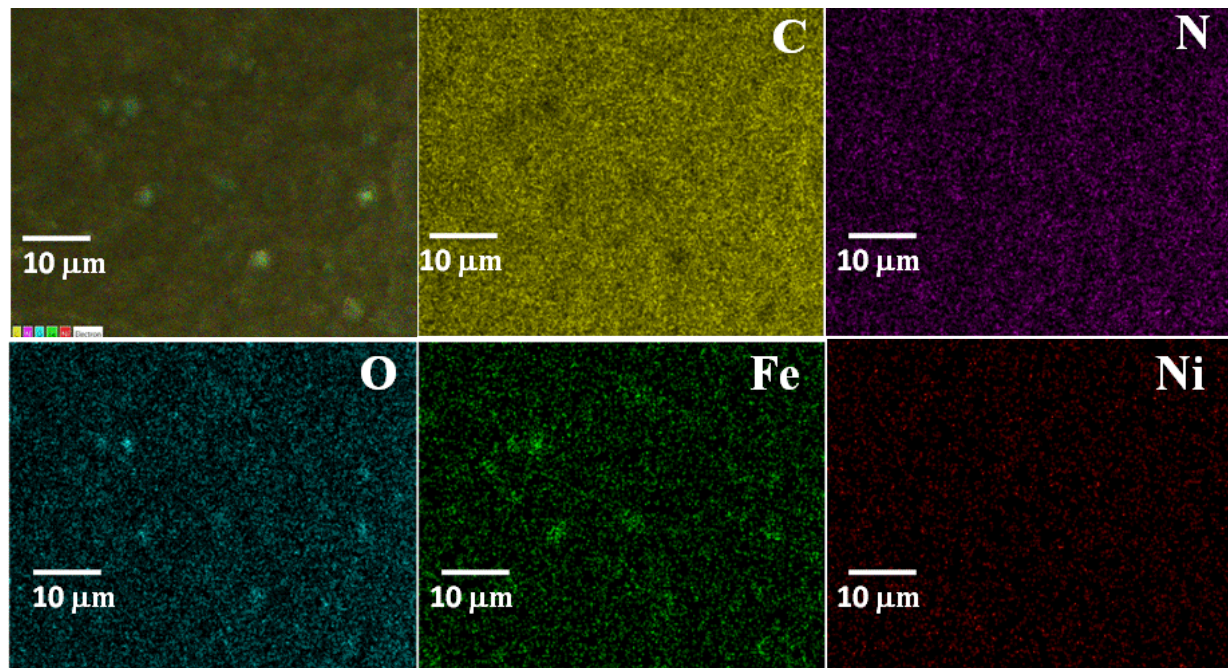


Fig. S 2 SEM-EDX elemental mapping of the synthesized NiFe (1:1)-dried gel.

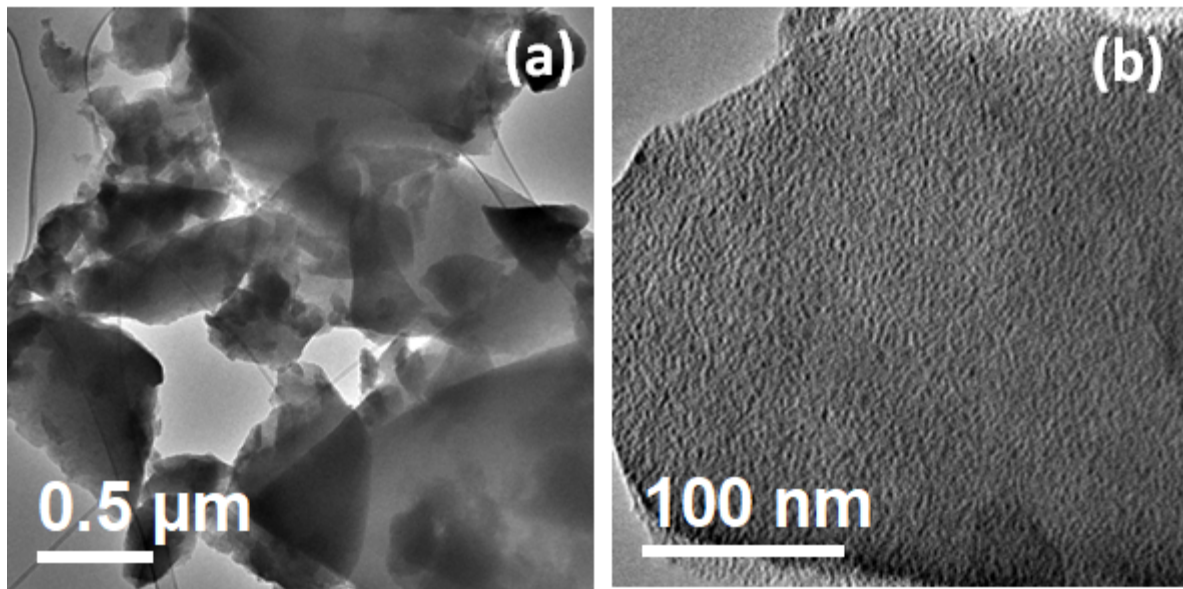


Fig. S3 TEM images of NiFe(1:1)-Gel.

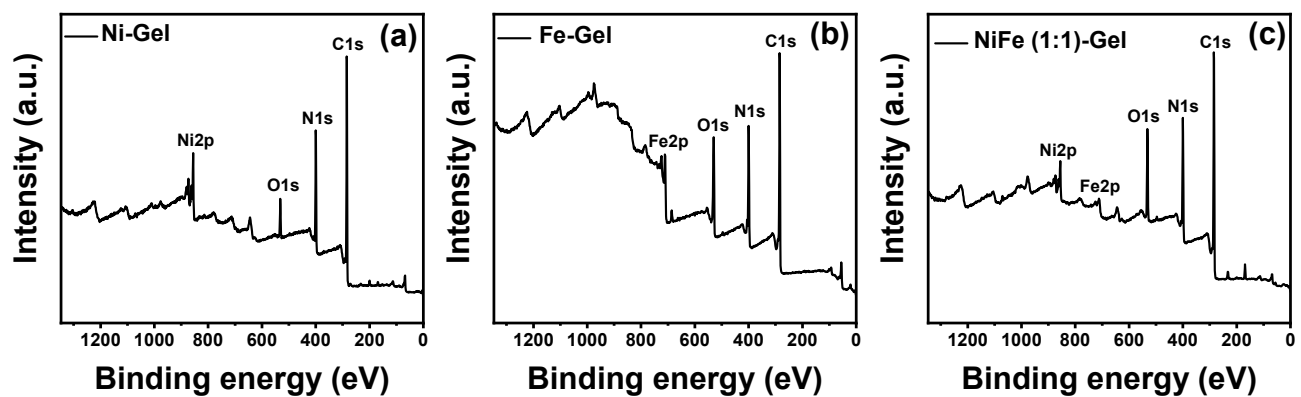


Fig. S4 XPS survey spectra of a) Ni-Gel b) Fe-Gel and c) NiFe(1:1)-Gel.

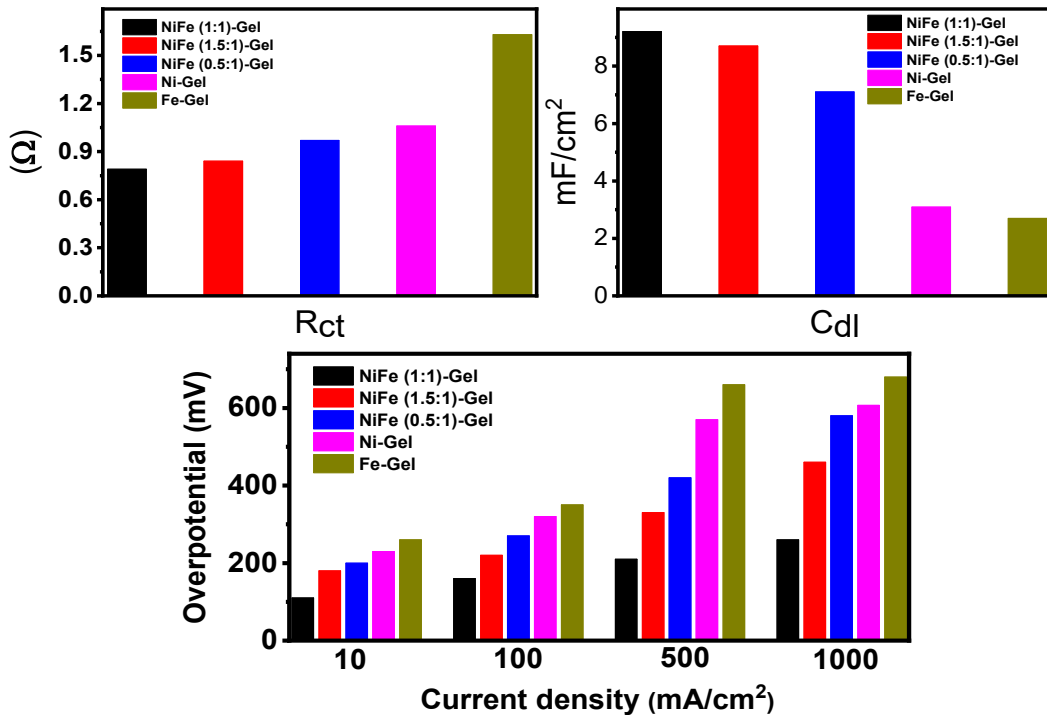


Fig. S5 Summarized OER properties in bar diagram of different samples.

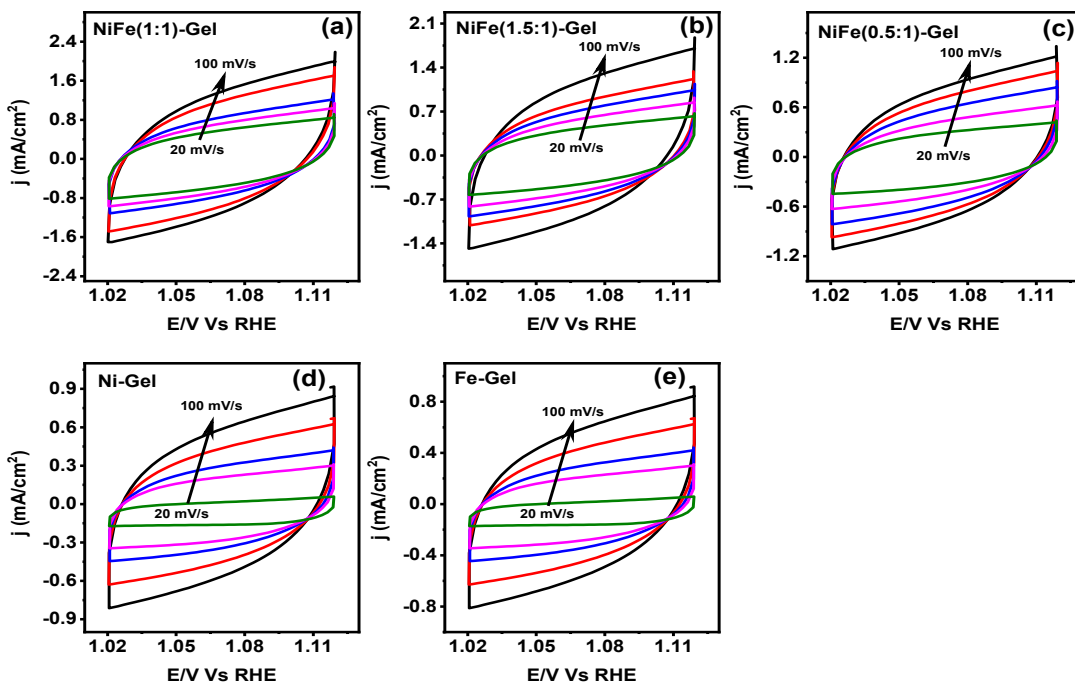


Fig. S6 CV curves with varying scan rate of 20, 40, 60, 80, 100 mV S⁻¹ of (a) NiFe(1:1)-Gel (b) NiFe(1.5:1)-Gel (c) NiFe(0.5:1)-Gel (d) Ni-Gel and (e) Fe -Gel.

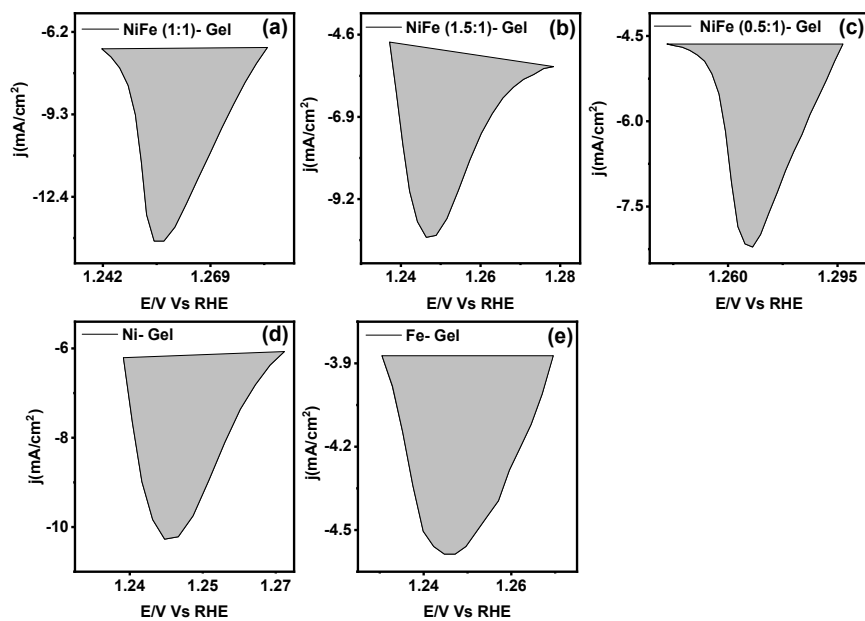


Fig. S7 The area of reduction peaks of the (a) NiFe(1:1)-Gel (b) NiFe(1.5:1)-Gel (c) NiFe(0.5:1)-Gel (d) Ni-Gel and (e) Fe -Gel.

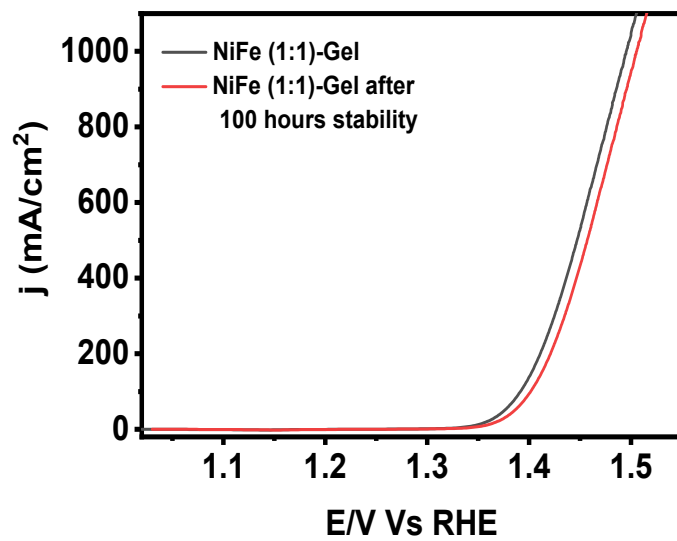


Fig. S8 LSV curve of NiFe(1:1)-Gel at initial and after 100 hours stability measurements for electrochemical OER experiment.

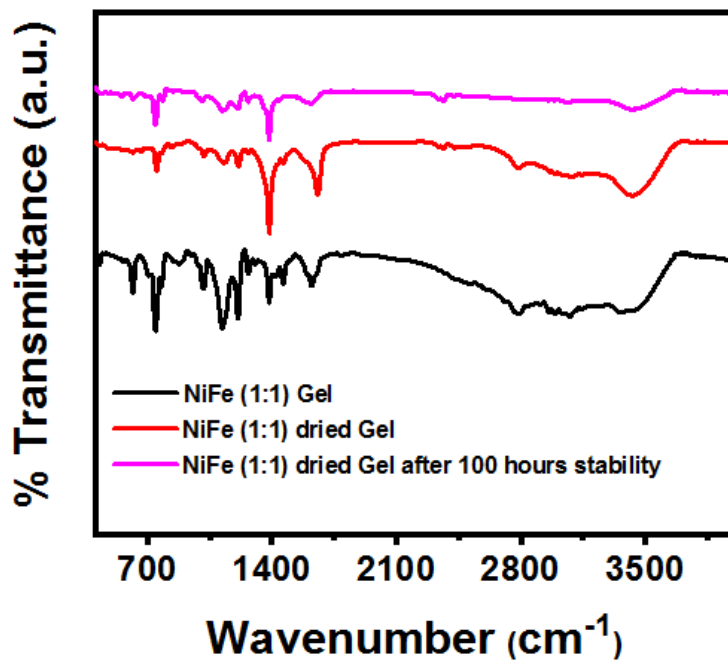


Fig. S9 FT-IR data of synthesized NiFe(1:1)-Gel, NiFe(1:1)-dried gel and after 100 hours stability of NiFe (1:1)- dried gel.

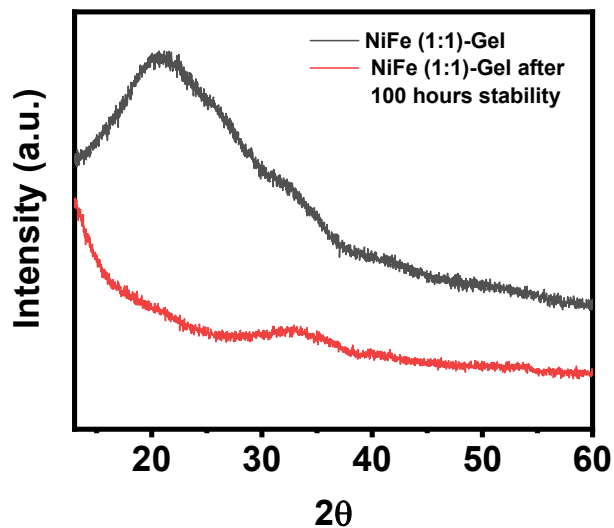


Fig. S10 XRD patterns of synthesized NiFe(1:1)-dried gel and after 100 hours stability of NiFe(1:1)- dried gel (After stability sample, collected from Carbon cloth).

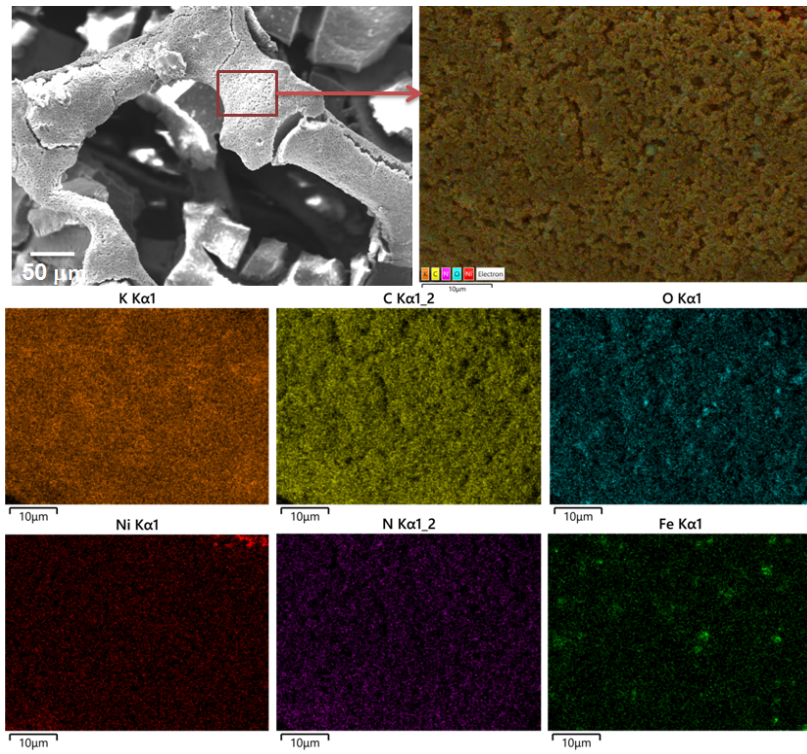


Fig. S11 SEM image and corresponding elemental mapping image of NiFe(1:1)-Gel after 100 hours of stability.

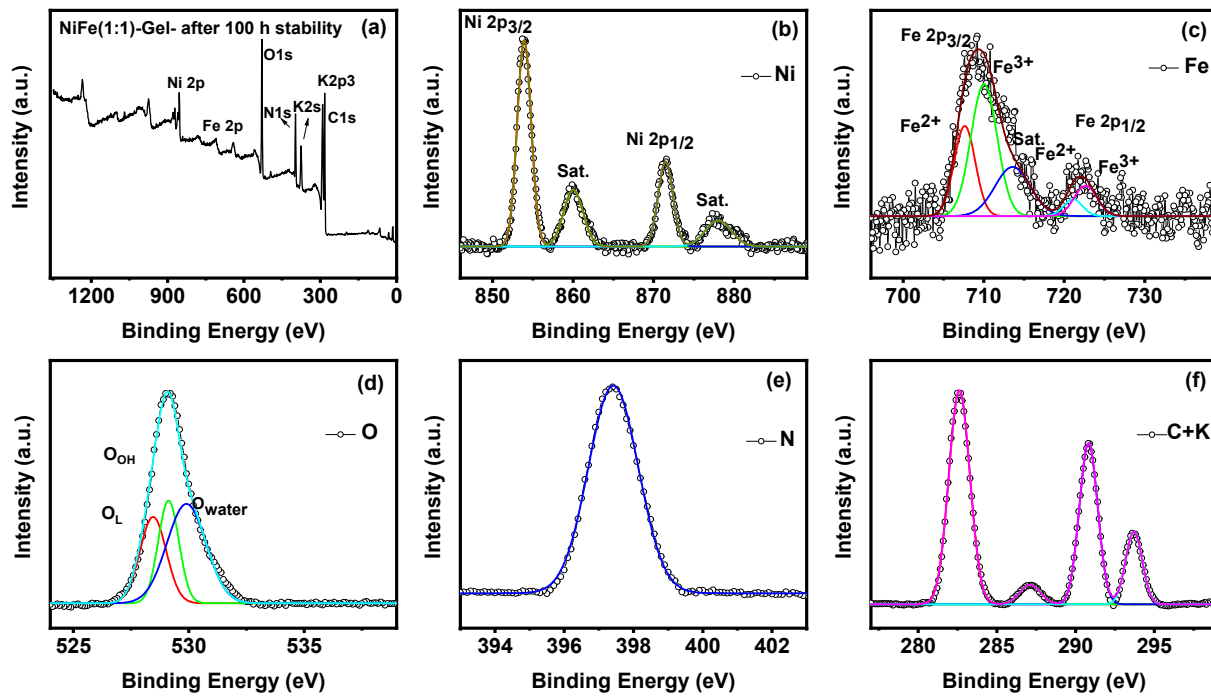


Fig. S12 XPS spectra of NiFe(1:1)-Gel after 100hours of three electrode OER chronoamperometry experiment at a fixed 1.49 V to attain the current density of 1000 mA/ cm² for 100 hours; XPS survey spectra (a), High-resolution Ni 2p (b), Fe 2p (c), O 1s (d), N 1s (e), and C 1s+K (f).

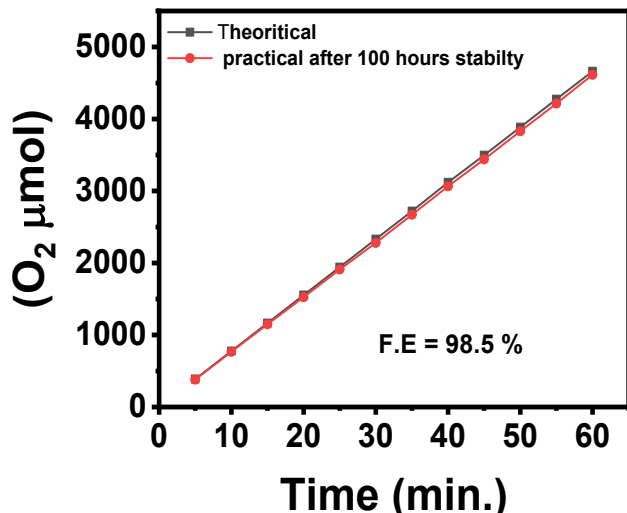


Fig. S13 Theoretical and measured faradaic efficiency after 100 hours stability of NiFe (1:1)-Gel.

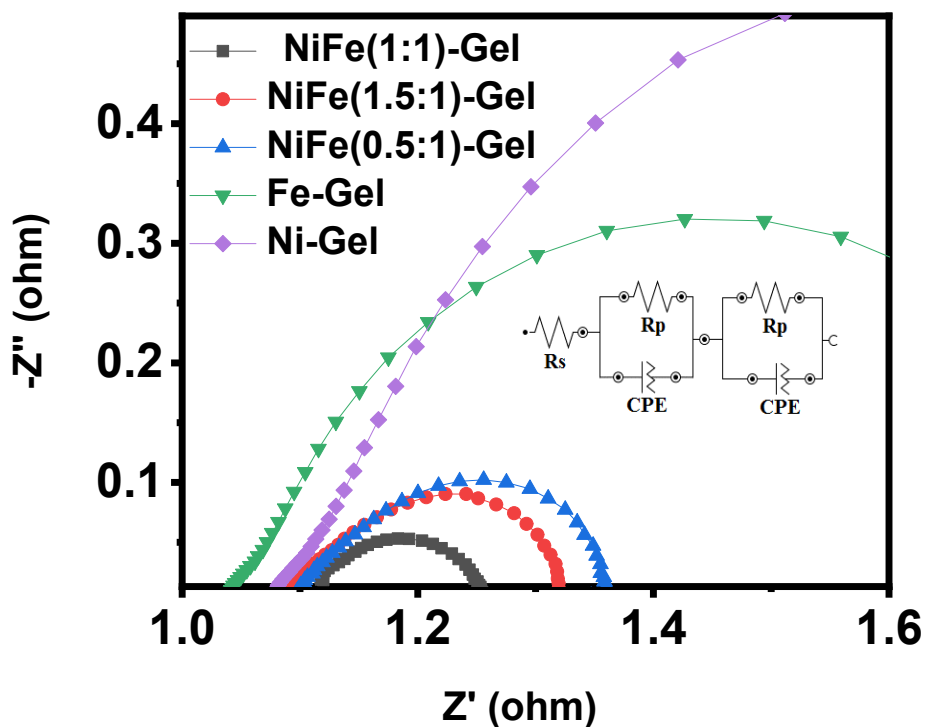


Fig. S14 Nyquist plot of NiFe(1:1)-Gel for HER.

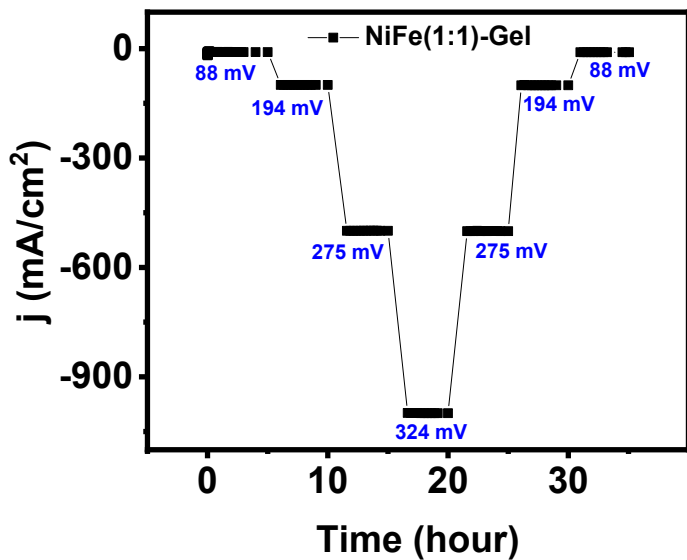


Fig. S15 HER chronoamperometric measurement as a function of current density of NiFe(1:1)-Gel.

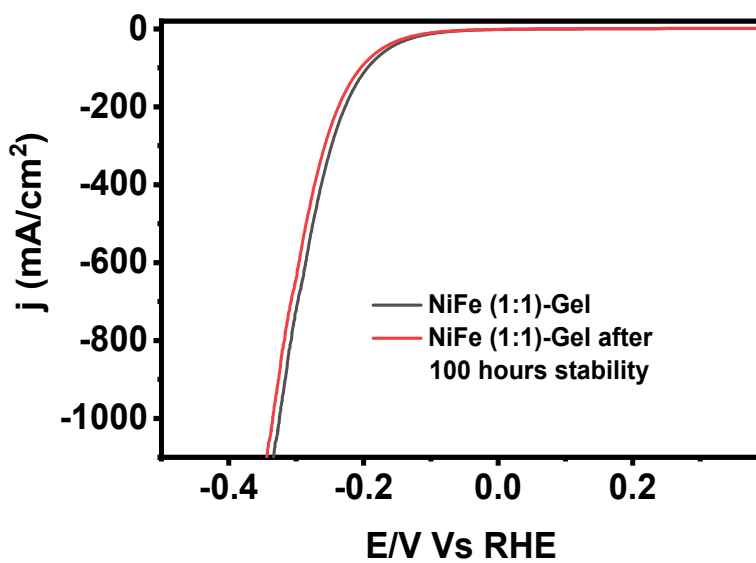


Fig. S16 LSV curve of NiFe(1:1)-Gel at initial and after 100 hours stability measurements for electrochemical HER experiment.

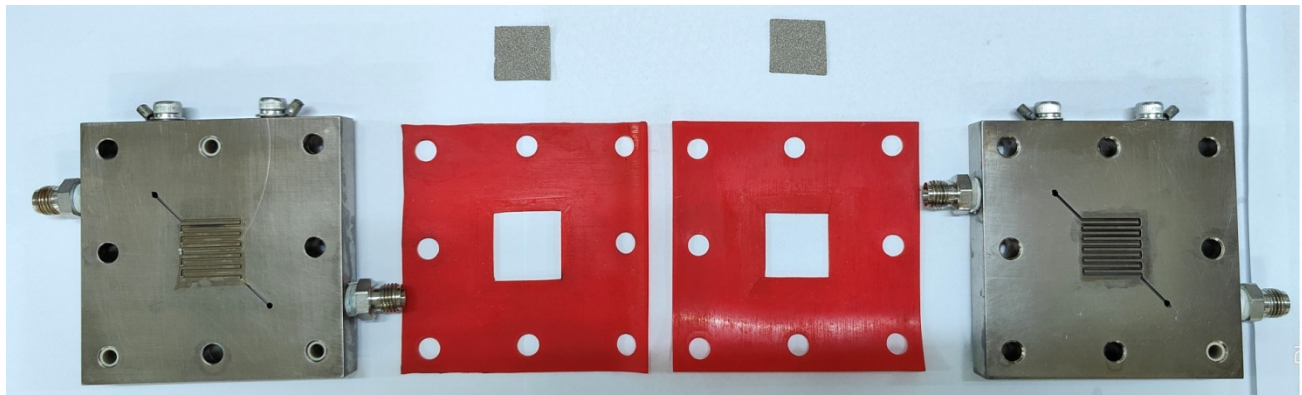


Fig. S17 Photograph of the (2cm×2cm) AEM electrolyser.

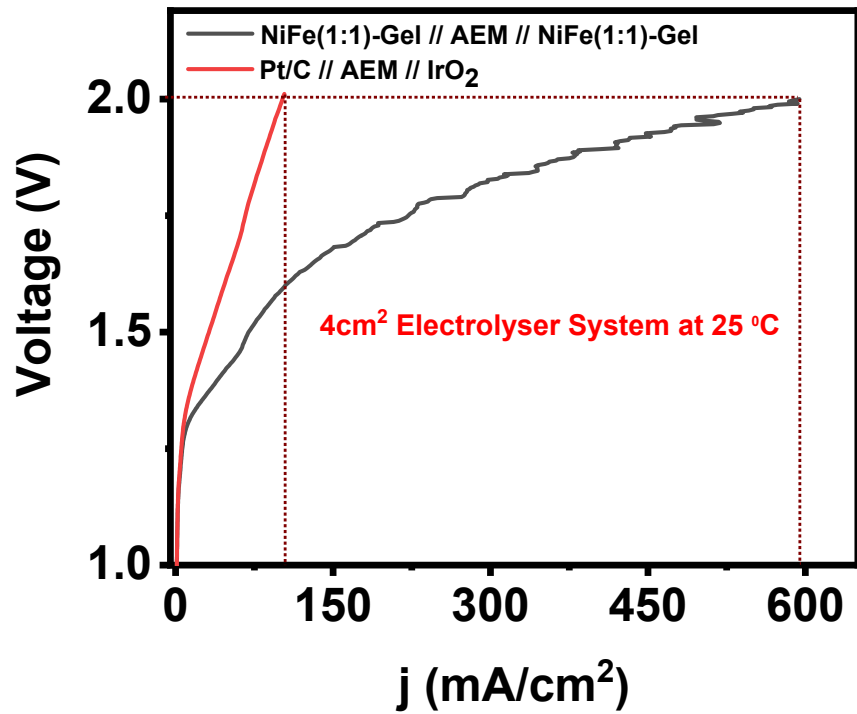


Fig. S18 LSV curve of NiFe(1:1)-Gel // AEM // NiFe(1:1)-Gel and Pt/C // AEM // IrO $_2$ of 4 cm 2 electrolyser system at 25 °C

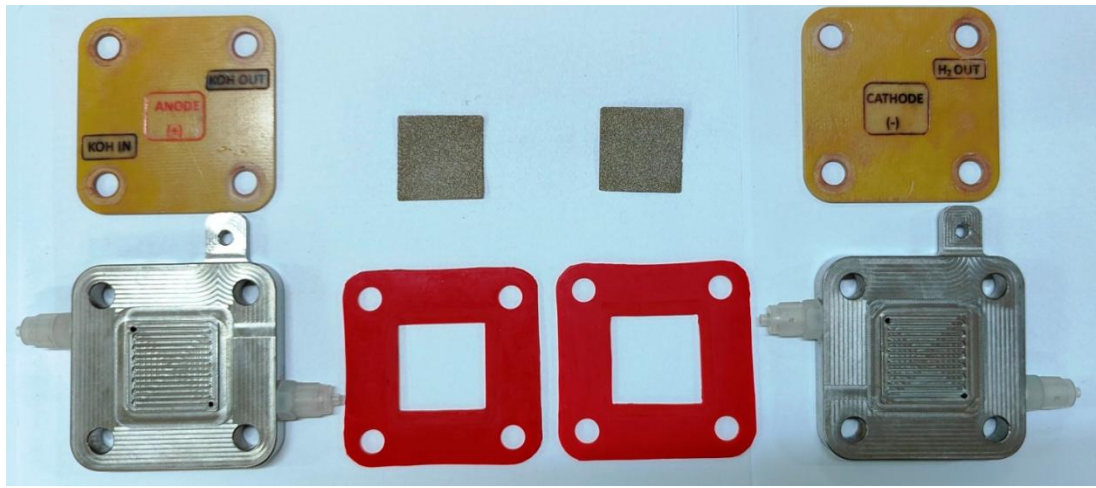


Fig. S19 Photograph of the (3cm×3cm) AEM electrolyser.

Other Supporting Tables

Table S4. A comparison of electrochemical OER activity of synthesized NiFe (1:1)-Gelwith literature reported PGM free transition metal based catalysts.

S. No	Catalyst	η_x Overpotential (mV)					Tafel (mV/dec)	Reference
		η_{10}	η_{50}	η_{100}	η_{500}	η_{1000}		
1	NiFe (1:1)-Gel	110		160	210	260	29	This work
2	Mo ₂ S ₃ @NiMo ₃ S ₄	173			350	390	33.7	S-1
3	Ni _{0.8} Fe _{0.2} -AHN	200			240	260	34.7	S-2
4	NiMoN@NiFeN	210			337	398	58.6	S-3
5	Ni ₂ P-Fe ₂ P/NF	220			290	340	58	S-4
6	Co ₄ N-CeO ₂	239				491	37.1	S-5
7	NiMoO _x /NiMoS	186			290	334	34	S-6
8	LiCoBPO	216			324	470	60	S-7
9	FeP/Ni ₂ P	154			210	290	22.7	S-8
10	CoMoS _x /NF	334				442	53	S-9
11	NiSe@NiOOH		332	~420*			162	S-10
12	Ni ₃₂ Fe oxide	291					58	S-11
13	Fe(0.5)-doped β -Ni(OH) ₂	260					32	S-12
14	S-NiFe ₂ O ₄	267					36.7	S-13
15	Fe ₁₁ NiO		259				49.4	S-14
16	NiCoFe _x P			290			56	S-15
17	NiFe LDH	280					49.4	S-16
18	Ni–Fe(O _x H _y)	298					37	S-17
19	NiFe LDH/NiCo ₂ O ₄	290					53	S-18
29	Fe ₃ O ₄ /NiC _x			308	398		63	S-19
21	Cu ₂ O		375*	400*			90	S-20

*Estimated data obtained from respective polarisation curves

Table S5. A comparison of electrochemical HER activity of synthesized NiFe(1:1)-gel with literature reported PGM free transition metal based catalysts.

S. No	Electrocatalyst	Electrolyte	η_x Overpotential (mV)	Tafel (mV/dec)	Reference
.

			η_{10}	η_{100}	η_{500}	η_{1000}	
1	NiFe(1:1)-gel	1 M KOH	88	194	275	324	72
2	NiFeMo-P-C	1 M KOH	87				87.3
3	NiFeAu LDH	1 M KOH	89	192			90
4	NiFe-Ru-LDHNS	1 M KOH	29				31
5	$\text{Ni}_{1-x}\text{Fe}_x\text{-LDH}$	1 M KOH	170	290*			83
6	$\text{Ni}_{0.75}\text{Fe}_{0.125}\text{V}_{0.125}\text{-LDHs/NF}$	1 M KOH	125	230*			62
7	NiCo-LDH/NF	1 M KOH	162	392*			141
8	Ni-doped MoS ₂ nanosheets	1 M KOH	98				32
9	NiS ₂ NWs/CFP	1 M KOH	165	300*			134
10	Ce@NiFe-LDH	1 M KOH	81	180*	240*		80.94
11	SV-MoS ₂	1 M KOH	170				60
12	Ni ₂ P-Fe ₂ P/NF	1 M KOH		208*	299*	330	65
13	CoMoSx/NF	1 M KOH	89	198*	269		94

* Estimated data obtained from respective polarization curves

Table S6. Comparison of water-splitting performances for NiFe(1:1)-Gel with reported bifunctional electrocatalysts in the alkaline media.

S.No	Catalyst	Current density	Voltage	Reference
1	NiFe(1:1)-gel	10 mA cm⁻²	1.49 V	This work
2	NiCoFeMnCrP	10 mA cm ⁻²	1.32 V	S-33

3	N-Co ₃ O ₄ @C@NF	10 mA cm ⁻²	1.40 V	S-34
4	Fe _{0.09} Co _{0.13} -NiSe ₂	10 mA cm ⁻²	1.52 V	S-35
5	Ni ₃ N-NiMoN-5	10 mA cm ⁻²	1.54 V	S-36
6	CoSn ₂	10 mA cm ⁻²	1.55 V	S-37
7	Co ₂ P NC	10 mA cm ⁻²	1.56 V	S-38
8	W ₂ N/WC	10 mA cm ⁻²	1.58 V	S-39
9	NiCoP	10 mA cm ⁻²	1.59 V	S-40
10	3DSe(NiCo)Sx/(OH)x	10 mA cm ⁻²	1.6 V	S-41
11	NC@CuCo ₂ Nx/CF	10 mA cm ⁻²	1.62 V	S-42
12	δ-FeOOH NSs/NF	10 mA cm ⁻²	1.62 V	S-43
13	Ni-Co-P HNBs	10 mA cm ⁻²	1.62 V	S-44
14	Co/b-Mo ₂ C@N-CNTs	10 mA cm ⁻²	1.64 V	S-45
15	Co/CNFs (1000)	10 mA cm ⁻²	1.69 V	S-46
16	Co(OH) ₂ @NCNTs@NF	10 mA cm ⁻²	1.72 V	S-47
17	Fe ₃ C-Co/NC	10 mA cm ⁻²	1.77 V	S-48
18	c/a-NiCoMoP	10 mA cm ⁻²	1.57 V	S-49
19	Co _{0.85} Se/NC	10 mA cm ⁻²	1.7 V	S-50
20	CoFeP@C	10 mA cm ⁻²	1.55 V	S-51
21	N,Ce-NiCoP/NF	10 mA cm ⁻²	1.54 V	S-52
22	Ni ₂ P-CoCH/CFP	10 mA cm ⁻²	1.53 V	S-53

Table S7. Comparison of water-splitting performances for NiFe(1:1)-Gel with reported AEM electrolyser system.

S. No.	Catalyst	Electrolyte	Current density (mAcm ⁻²) in 2V	Reference
1	NiFe(1:1)-Gel	1M KOH	588	This work

	Pt/C AEM IrO₂	1M KOH	103	This work
3	Mn ₃ O ₄ @CeO ₂ /γ-FeOOH AEM Mn ₃ O ₄ @CeO ₂ /γ-FeOOH	1M KOH	366	S-54
4	NiCoTi/Ti AEM NiCoTi/Ti	1M KOH	180	S55
5	NiCo/r-GO AEM Co ₃ O ₄ /r-GO	1M KOH	105	S56
6	CuCoO AEM Ni	1M KOH	156	S57
7	Cu _x Co _{3-x} O ₄ AEM Ni	1M KOH	100	S58
8	NiCo ₂ O ₄ /Ni AEM Ni	1M KOH	106	S59
9	γ-FeOOH-NS AEM γ-FeOOH-NS	1M KOH	209	S60

References.

- S1 T. Wu, S. Xu, Z. Zhang, M. Luo, R. Wang, Y. Tang, J. Wang and F. Huang, *Adv. Sci.*, 2022, **9**, 2202750.

- S2 C. Liang, P. Zou, A. Nairan, Y. Zhang, J. Liu, K. Liu, S. Hu, F. Kang, H. J. Fan and C. Yang, *Energ. Environ. Sci.*, 2020, **13**, 86
- S3 L. Yu, Q. Zhu, S. Song, B. McElhenny, D. Wang, C. Wu, Z. Qin, J. Bao, Y. Yu, S. Chen and Z. Ren, *Nat. Commun.* 2019, **10**, 5106.
- S4 L. Wu, L. Yu, F. Zhang, B. McElhenny, D. Luo, A. Karim, S. Chen and Z. Ren, *Adv. Funct. Mater.*, 2021, **31**, 2006484.
- S5 H. Sun, C. Tian, G. Fan, J. Qi, Z. Liu, Z. Yan, F. Cheng, J. Chen, C-P. Li and M. Du, *Adv. Funct. Mater.*, 2020, **30**, 1910596.
- S6 P. Zhai, Y. Zhang, Y. Wu, J. Gao, B. Zhang, S. Cao, Y. Zhang, Z. Li, L. Sun and J. Hou, *Nat. Commun.* 2020, **11**, 5462.
- S7 P. W. Menezes, A. Indra, I. Zaharieva, C. Walter, S. Loos, S. Hoffmann, R. Schlögl, H. Dau and M. Driess, *Energ. Environ. Sci.*, 2019, **12**, 988.
- S8 F. Yu, H. Zhou, Y. Huang, J. Sun, F. Qin, J. Bao, W. A. Goddard III, S. Chen and Z. Ren, *Nat. Commun.*, 2018, **9**, 2551.
- S9 X. Shan, J. Liu, H. Mu, Y. Xiao, B. Mei, W. Liu, G. Lin, Z. Jiang, L. Wen and L. Jiang, *Angew. Chem. Int. Ed.*, 2020, **59**, 1659.
- S10 X. Li, G.-Q. Han, Y.-R. Liu, B. Dong, W.-H. Hu, X. Shang, Y.-M. Chai, and C.-G. Liu, *ACS Appl. Mater. Interfaces.*, 2016, **8**, 20057–20066.
- S11 M. Yu, G. Moon, E. Bill, and H. Tuysuz, *ACS Applied Energy Materials*, 2019, **2**, 1199–1209.
- S12 K. Zhu, H. Liu, M. Li, X. Li, J. Wang, X. Zhu and W. Yang, *J. Mater. Chem. A*, 2017, **5**, 7753–7758.
- S13 J. Liu, D. Zhu, T. Ling, A. Vasileff, S.-Z. Qiao, *Nano Energy*, 2017, **40**, 264–273.
- S14 Z. Wu, Z. Zou, J. Huang, F. Gao, *J. Catal.*, 2018, **358**, 243–252.
- S15 C. Ray, S. C. Lee, B. Jin, A. Kundu, J. H. Park, and S. C. Jun, *ACS Sus. Chem. Eng.*, 2018, **6**, 6146–6156.
- S16 L. Yu, J. F. Yang, B. Y. Guan, Y. Lu, X. W. D. Lou, *Angew. Chem. Int. Ed.*, 2018, **57**, 172–176.
- S17 M. Gorlin, P. Chernev, P. Paciok, C.-W. Tai, J. F. de Araújo, T. Reier, M. Heggen, R. D.-Borkowski, P. Strasser and H. Dau, *Chem. Commun.*, 2019, **55**, 818–821

- S18 Z. Wang, S. Zeng, W. Liu, X. Wang, Q. Li, Z. Zhao, and F. Geng, *ACS Appl. Mater. Interf.*, 2017, **9**, 1488–1495.
- S19 H. Zhang, S. Geng, M. Ouyang, H. Yadegari, F. Xie and D.J. Riley, *Adv. Sci.*, 2022, **9**, 2200146 (1–15).
- S20 H. Wang, J. Ying, Y.X. Xiao, J.B. Chen, J.H. Li, Z.Z. He, H.J. Yang, X.Y. Yang, *Electrochim. Commun.*, 2022, **134**, 107177.
- S21. X. Zhou, T. Yang, T. Li, Y. Zi, S. Zhang, L. Yang, Y. Liu, J. Yang, and J. Tang, *Nano Res. Energy.*, 2023, **2**, e9120086
- S22. X. P. Li, W. K. Han, K. Xiao, T. Ouyang, N. Li, F. Peng and Q. Liu, *Catal. Sci. Technol.*, 2020, **10**, 4184–4190.
- S23. G. Chen, T. Wang, J. Zhang, P. Liu, H. Sun, X. Zhuang, M. Chen and X. Feng, *Adv. Mater.*, 2018, **30**, 1–7.
- S24. G. Rajeshkhanna, T. I. Singh, N. H. Kim and J. H. Lee, *ACS Appl. Mater. Interfaces*, 2018, **10**, 42453–42468.
- S25. K. N. Dinh, P. Zheng, Z. Dai, Y. Zhang, R. Dangol, Y. Zheng, B. Li, Y. Zong and Q. Yan, *Small*, 2018, **14**, 1-9.
- S26. W. Liu, J. Bao, M. Guan, Y. Zhao, J. Lian, J. Qiu, L. Xu, Y. Huang, J. Qian and H. Li, *Dalt. Trans.*, 2017, **46**, 8372–8376.
- S27. J. Zhang, T. Wang, P. Liu, S. Liu, R. Dong, X. Zhuang, M. Chen and X. Feng, *Energy Environ. Sci.*, 2016, **9**, 2789–2793
- S28. Y. Guo, D. Guo, F. Ye, K. Wang and Z. Shi, *Int. J. Hydrogen Energy* 2017, **42**, 17038–17048
- S29. S. Nagappan, A. Karmakar, R. Madhu, H. N Dhandapani, K. Bera, A. De and S. Kundu, *ACS Appl. Energy Mater.*, 2022, **5**, 12768–12781
- S30. H. Li, C. Tsai, A. L. Koh, L. Cai, A. W. Contryman, A. H. Fragapane, J. Zhao, H. Han, H. C. Manoharan, F. A. Pedersen, J. K. Nørskov and X. Zheng, *Nat. Mater.*, 2016, **15**, 48–53.
- S31. L. Wu, L. Yu, F. Zhang, B. McElhenny, D. Luo, A. Karim, S. Chen and Z. Ren, *Adv. Funct. Mater.*, 2021, **31**, 2006484-2006496
- S32. L. Wen, X. Shan, J. Liu, H. Mu, Y. Xiao, B. Mei, W. Liu, G. in, Z. Jiang, and L. Jiang, *Angew. Chem. Int. Ed.* 2020, **59**, 1659–1665
- S33. D. Lai, Q. Kang, F. Gao and Q. Lu, *J. Mater. Chem. A*, 2021, **9**, 17913–17922

- S34. Y. Ha, L. Shi, Z. Chen and R. Wu, *Adv. Sci.*, 2019, **6**, 1900272.
- S35. Y. Sun, K. Xu, Z. Wei, H. Li, T. Zhang, X. Li, W. Cai, J. Ma, H. J. Fan and YLi, *Adv. Mater.*, 2018, **30**, 1802121.
- S36. P. Ge, C. Zhang, H. Hou, B. Wu, L. Zhou, S. Li, T. Wu, J. Hu, L. Mai and X. Ji, *Nano Energy*, 2018, **44**, 353.
- S37. P. W. Menezes, C. Panda, S. Garai, C. Walter, A. Guiet and M. Driess, *Angew. Chem. Int. Ed.*, 2018, **57**, 15237
- S38. H. Li, Q. Li, P. Wen, T. B. Williams, S. Adhikari, C. Dun, C. Lu, D. Itanze, L. Jiang, D. L. Carroll, G. L. Donati, P. M. Lundin, Y. Qiu and S. M. Geyer, *Adv. Mater.*, 2018, **30**, 1705796.
- S39. J. Diao, Y. Qiu, S. Liu, W. Wang, K. Chen, H. Li, W. Yuan, Y. Qu and X. Guo, *Adv. Mater.*, 2020, **32**, 1905679
- S40. V. R. Jothi, R. Bose, H. Rajan, C. Jung and S. C. Yi, *Adv. Energy Mater.*, 2018, **8**, 1802615.
- S41. C. Hu, L. Zhang, Z. J. Zhao, A. Li, X. Chang and J. Gong, *Adv. Mater.*, 2018, **30**, 1705538.
- S42. J. Zheng, X. Chen, X. Zhong, S. Li, T. Liu, G. Zhuang, X. Li, S. Deng, D. Mei and J. G. Wang, *Adv. Funct. Mater.*, 2017, **27**, 1704169.
- S43. B. Liu, Y. Wang, H. Q. Peng, R. Yang, Z. Jiang, X. Zhou, C. S. Lee, H. Zhao and W. Zhang, *Adv. Mater.*, 2018, **30**, 1803144.
- S44. Y. Y. Ma, Z. L. Lang, L. K. Yan, Y. H. Wang, H. Q. Tan, K. Feng, Y. J. Xia, J. Zhong, Y. Liu, Z. H. Kang and Y. G. Li, *Energy Environ. Sci.*, 2018, **11**, 872.
- S45. T. Ouyang, Y. Q. Ye, C. Y. Wu, K. Xiao and Z. Q. Liu, *Angew. Chem. Int. Ed.*, 2019, **58**, 4923.
- S46. Z. Yang, C. Zhao, Y. Qu, H. Zhou, F. Zhou, J. Wang, Y. Wu and Y. Li, *Adv. Mater.*, **31**, 2019, 1808043.
- S47. X. Nie, B. Ji, N. Chen, Y. Liang, Q. Han and L. Qu, *Nano Energy*, 2018, **46**, 297–304.
- S48. C. C. Yang, S. F. Zai, Y. T. Zhou, L. Du and Q. Jiang, *Adv. Funct. Mater.*, 2019, **29**, 1901949.
- S49. B. Wei, N. Zhang, L. Huang, Y. Xue, X. Zhou, R. Jiang, *ACS Appl. Energy Mater.*, 2024, **7**, **11**, 5018–5027.
- S50. W. W. Tian, Y. D. Ying, J. T. Ren and Z. Y. Yuan, *J. Mater. Chem. A.*, 2023, **11**, 8024.
- S51. W. W. Tian, Y. D. Ying, J. T. Ren and Z. Y. Yuan, *Adv. Energy Mater.*, 2022, **12**, 2202394.
- S52. H. Wang, L. Yu, J. Peng, J. Zou, W. Gong & J. Jiang, *Nano Res.*, 2024, **17**, 282

- S53. S. Zhang, C. Tan, R. Yan, X. Zou, F. L. Hu, Y. Mi, C. Yan and S. Zhao, *Angew. Chem. Int. Ed.*, 2023, **62**, e202302795
- S54. D. Ghosh, D. K. Bora and A. B. Panda, *J. Mater. Chem. A*, 2024, **12**, 30783-30797.
- S55. P. Anesan, A. Sivanantham and S. Shanmugam, *ACS Appl. Mater. Interfaces*, 2017, **14**, 12416.
- S56. S. Kamali, M. Zhiani and H. Tavakol, *Renew Energ.*, 2020, **154**, 1122.
- S57. E. Lopez-Fernandez, J. Gil-Rostra, C. Escudero, I. J. Villar-Garcia, F. Yubero, A. D. Consuegra and A. R. Gonzalez-Elipe, *J. Power Sources*, 2021, **485**, 229217.
- S58. E. L.-Fernandez, J. G.-Rostra, J. P. Espinos, A. R. G.-Elipe, F. Yubero and A. de Lucas-Consuegra, *J. Power Sources*, 2019, **415**, 136.
- S59. D. Chanda, J. Hnat, T. Bystron, M. Paidar, K. Bouzek, *J. Power Sources*, 2017, **347**, 247.
- S60. D. K. Bora, D. Ghosh, A. Jana, R. K. Nagarale and A. B. Panda, *ACS Appl. Eng. Mater.*, 2024, **2**, 975-987